CMS Physics Analysis Summary

Contact: cms-pag-conveners-fsq@cern.ch 2013/05/14

Azimuthal angle decorrelations of jets widely separated in rapidity in pp collisions at $\sqrt{s} = 7$ TeV

The CMS Collaboration

Abstract

The azimuthal angle decorrelations of jets most forward and backward in rapidity (Mueller-Navelet jets) are measured with data collected in pp collisions with the CMS detector at the LHC at $\sqrt{s} = 7$ TeV. The azimutal angle distributions, average cosines of the difference in azimuthal angle between Mueller-Navelet jets, and ratios of the cosines are measured for jets with $p_{\mathrm{T}} > 35$ GeV and $|y| < 4.7$. The results are presented as a function of the rapidity separation Δy between jets, reaching a Δy up to 9.4 for the first time. The results are compared to predictions of various Monte-Carlo event generators and analytical predictions based on the DGLAP and BFKL parton evolution schemes. The measurements are also used to investigate effects of parton showering and multiparton interactions.

1 Introduction

QCD is well tested in hard processes ($\sqrt{s} \geq p_{\mathrm{T}} \gg \Lambda_{QCD}$) and the data are successfully described by perturbative QCD (pQCD) calculations within the framework of collinear factorization and Dokshitzer-Gribov-Lipatov-Altarelli-Parisi (DGLAP) evolution equations [1–5]. The study of the dynamics of hadron jets in proton-proton collisions yields important information about underlying partonic processes. Parton-parton scattering at leading order in the strong coupling α_s produces two outgoing partons which are back-to-back in the azimuthal plane. The partons manifest themselves as a collimated stream of hadrons, which are the observable jets. A deviation from the back-to-back configuration occurs if higher order parton contributions are considered, which can be described by the parton showers initiated by the initial and final partons in the scattering process.

At high centre-of-mass energies a kinematical domain can be reached where semi-hard parton interactions ($\sqrt{s} \gg p_{\mathrm{T}} \gg \Lambda_{QCD}$) play a substantial role. The asymptotic region, where $\sqrt{s} \to \infty$ is described by Balitsky-Fadin-Kuraev-Lipatov (BFKL) equation [6–8]. Such a scenario might be approximated experimentally in pp collisions by requiring jets of similar p_{T} but highly separated in rapidity [9], The requirement of 2 jets with similar p_{T} suppresses contributions in the DGLAP scheme, which is based on p_{T} ordering. The azimuthal decorrelation of jets with large rapidity separation might therefore show effects beyond the DGLAP description. In a kinematic region, where semi-hard parton interactions are important, the azimuthal angle decorrelations will increase [10, 11] with increasing rapidity separation $\Delta y = |y_1 - y_2|$ between the jets, where y_1, y_2 are rapidities of the most forward and the most backward jets (Mueller-Navelet dijets, MN) [9].

Earlier searches for BFKL effects in hadron-hadron collisions and events with jets widely separated in rapidity were made at the Tevatron by the D0 experiment [12, 13]. The D0 measurements of azimuthal angle decorrelations were restricted to a rapidity separation $\Delta y < 6$, and no noticeable indications of BFKL effects were found [12]. Studies of the collision energy dependence of dijet production at large rapidity intervals have found a strong dependence on collision energy [13].

Recently ATLAS [14] and CMS [15] released measurements of dijet production in pp collisions at 7 TeV as a function of rapidity separation between jets. The measurements show that the BFKL effects are not dominant for jets with $p_{\mathrm{T}} > 35$ GeV at collision energy of 7 TeV.

In this paper observables connected to the azimuthal angle decorrelation of MN dijets are presented.

2 Physics Motivation and Monte Carlo event generators

The normalised cross section as a function of the azimuthal angle difference, $\Delta\phi$ between MN jets with $p_{\mathrm{T}} > p_{\mathrm{Tmin}}$ can be written as a Fourier series

$$\frac{1}{\sigma}\frac{d\sigma}{d(\Delta\phi)}(\Delta y, p_{\mathrm{Tmin}}) = \frac{1}{2\pi}\left[1 + 2\sum_{n=1}^{\infty} C_n(\Delta y, p_{\mathrm{Tmin}}) \cdot cos(n(\pi - \Delta\phi))\right], \quad (1)$$

The Fourier coefficients $C_n(\Delta y, p_{\mathrm{Tmin}})$ are equal to the average cosines of the decorrelation angle: $C_n(\Delta y, p_{\mathrm{Tmin}}) = \langle cos(n(\pi - \Delta\phi))\rangle$, where $\Delta\phi = \phi_1 - \phi_2$ is the difference between the azimuthal angles ϕ_1 and ϕ_2 of the jets most forward and backward in rapidity.

If there are only two jets in final state, then they have to be back-to-back ($\Delta\phi = \pi$) in the azimuthal plane and the average cosines equal unity: $\langle cos(n(\pi - \Delta\phi))\rangle = 1$. Due to parton

radiation the width of the azimuthal distribution is driven by Fourier harmonics involving $\langle cos(n(\pi - \Delta\phi))\rangle$. According to the BFKL approach, the number of emitted partons increases with increasing rapidity interval between the MN jets and, hence, the MN jets are no longer back-to-back in azimuth leading to a decorrelation:

$\langle cos(n(\pi - \Delta\phi))\rangle < 1.$

Parton-parton scattering in the DGLAP approach should not exhibit strong decorrelation effects as a function of Δy, therefore the observation of such decorrelations could indicate the presence of BFKL contributions.

In this paper the average cosines of the azimuthal angle between MN jets, $(\pi - \Delta\phi)$, $2(\pi - \Delta\phi)$ and $3(\pi - \Delta\phi)$, as suggested in Refs. [10, 11, 16–19], have been measured as a function of rapidity separation Δy. In addition, the ratios of the average cosines C_2/C_1 and C_3/C_2 are measured, as proposed in Refs. [17–19]. The average cosines reflect special conformal properties of BFKL-evolution equation [20], which are absent in DGLAP evolution. Moreover, in the ratios one can expect a suppression of DGLAP contributions [18], hence, the ratios will be sensitive to manifestations of BFKL-effects. In addition, in the ratios uncertainties related with factorization, renormalization scales are reduced [21].

The measurements were performed with the CMS detector in proton-proton collisions at $\sqrt{s} =$ 7 TeV for jets with $p_{\mathrm{T}} > 35$ GeV and $|y| < 4.7$ allowing a rapidity separation between the MN dijets of up to $\Delta y < 9.4$. The jets are defined with the anti-k$_T$ algorithm [22, 23] with jet size parameter $R = 0.5$. The minimal transverse momenta $p_{\mathrm{Tmin}} = 35$ GeV for the jets of the MN dijets were taken equal to avoid possible large effects related with factors $\log(p_{\mathrm{T1min}}/p_{\mathrm{T2min}})$ in the double-logarithm approximation.

The measured jet observables, corrected to stable particle level ($c\tau > 1$cm), are compared to predictions from various MC event generators applying the DGLAP approach in the leading logarithm (LL) approximation: PYTHIA 6 (version 6.422) [24] tune Z2 [25], HERWIG++ (version 2.5.1) tune UE-7000-EE-3 [26] and PYTHIA 8 (version 8.145) [27] tune 4C [28]. In addition PYTHIA 6 tune Z2 [25] without multiple parton interactions (MPI) as well as PYTHIA 6 tune Z2 [25] without polar angle ordering (AO) were used to investigate the sensitivity of the measured jet observables to the details of higher order parton contributions. The measurements are also compared to the DGLAP-based Monte Carlo generator SHERPA [29], which uses tree level $2 \to 2 + n$ matrix elements matched to LL parton showers (in this work n=0,1,2 was used). Finally, a comparison with CASCADE 2 generator [30], in which elements of BFKL approach in the LL approximation are implemented, and with full next-to-leading-logarithm (NLL) BFKL analytical predictions as obtained in Ref. [21] on the parton level is performed.

3 The CMS Detector

The component of the CMS detector [31] most relevant for this analysis is the calorimeter system extending to pseudorapidities $|\eta| = 5.0$, where $\eta = -\log[\tan(\theta/2)]$, and θ is the polar angle relative to the anticlockwise proton beam direction. The crystal electromagnetic calorimeter (ECAL) and the brass/scintillator hadronic calorimeter (HCAL) extend to pseudorapidities $|\eta| = 3.0$. The HCAL cells map to an array of ECAL crystals to form calorimeter towers projecting radially outwards from the nominal interaction point. The pseudorapidity region $3.0 < |\eta| < 5.0$ is covered by the hadronic forward (HF) calorimeter, which consists of steel absorber wedges with embedded radiation-hard quartz fibers, oriented parallel to the beam direction. The calorimeter towers in the barrel region have segmentation of $\Delta\eta \times \Delta\phi = 0.087 \times 0.087$,

becoming progressively larger in the endcap and forward regions ($\Delta\eta \times \Delta\phi = 0.175 \times 0.175$ at $\eta \sim 4.5$).

The CMS trigger system consists of a hardware Level-1 trigger and a software high-level trigger. Jets formed online by the trigger system use ECAL, HCAL and HF inputs for energy clustering and are not corrected for the jet energy response.

4 Event selection

Dijet events with a large rapidity separation are rare. Therefore, in addition to standard single-jet triggers, a dedicated trigger for forward-backward dijets was developed. This forward-backward-dijet trigger selected events with two jets in opposite hemispheres and $|\eta| > 3.0$, and jet raw transverse momentum $p_{\mathrm{T}} > 15\,\mathrm{GeV}$. It was operated with moderate prescaling, and the effective integrated luminosity recorded with it is $\simeq 5\,\mathrm{pb}^{-1}$. This resulted in the collection of a sample of large Δy dijet events 100 times larger than that collected with single-jet triggers alone.

The trigger efficiency was measured by means of a control sample selected with the minimum-bias trigger. The single-jet trigger was found to be 100% efficient for dijets with $p_{\mathrm{T}} > 35\,\mathrm{GeV}$. The single-jet trigger was also used for the determination of the efficiency of the forward-backward-dijet trigger. The latter was 100% efficient for dijets with $p_{\mathrm{T}} > 35\,\mathrm{GeV}$.

Jets were reconstructed offline from the energy depositions in the calorimeter towers, clustered with the anti-k$_T$ algorithm [22, 23] with jet size parameter $R = 0.5$. In the reconstruction process, the contribution from each tower was assigned a momentum, the absolute value and the direction of which were given by the energy measured in the tower, and the coordinates of the tower, respectively. The raw jet energy was obtained from the sum of the tower energies, and the raw jet momentum from the vectorial sum of the tower momenta. The raw jet energies were then corrected to establish a uniform relative response of the calorimeter in η and a calibrated absolute response in transverse momentum p_{T} [32]. The jet energy resolution for calorimeter jets with $p_{\mathrm{T}} \sim 35\,\mathrm{GeV}$ is about 22% for $|\eta| < 0.5$ and about 10% for $4 < |\eta| < 4.5$ [33]. The uncertainty of the jet energy calibration for jets with $p_{\mathrm{T}} \sim 35\,\mathrm{GeV}$ depends on η and is $\simeq 7 - 8\%$ [32].

In order to reduce the sensitivity to overlapping pp collisions (so-called "pile-up" events), events with only one primary vertex reconstructed within the luminous region were used for the measurement. The primary vertex is required to be present within ± 24 cm of the nominal interaction point along the beamline [34].

Loose jet quality cuts [35] were applied to suppress the effect of calorimeter noise. Events with at least two jets with $p_{\mathrm{T}} > 35\,\mathrm{GeV}$ and $|y| < 4.7$ where selected; only jets satisfying these criteria were used for the analysis.

A Mueller-Navelet dijet is defined as pair of jets passing the above criteria with largest rapidity separation in the event. The azimuthal angle difference $\Delta\phi$ between the two jets is measured in the range $0 < \Delta\phi < \pi$ for three bins of rapidity separations between jets: $\Delta y < 3.0$, $3.0 < \Delta y < 6.0$, $6.0 < \Delta y < 9.4$, normalised to unity integral. The average cosines $C_1 = \langle cos(\pi - \Delta\phi)\rangle$, $C_2 = \langle cos(2(\pi - \Delta\phi))\rangle$, $C_3 = \langle cos(3(\pi - \Delta\phi))\rangle$ are measured in bins of Δy up to 9.4. The cosine ratios C_3/C_2 and C_2/C_1 are calculated as ratios of average cosines for each bin in Δy.

5 Corrections

The finite jet p_T resolution results in jet p_T values at detector level that deviate from those at stable particle level. Due to the steep slope of the p_T spectrum, jets with smaller p_T may migrate to higher p_T, and thus increase the number of jets in distributions at the detector level. The finite jet η resolution and measurement offset lead to a finite Δy resolution and offset, such that dijets may migrate from one Δy bin to another.

Jets at stable particle level were obtained from the jets measured at the detector level by applying correction factors evaluated using Monte Carlo events generated with the PYTHIA 6 (version 6.422) Z2 tune and HERWIG++ (version 2.4.1 default tune). These were passed through the full CMS detector simulation based on GEANT 4 [36]. The simulations with PYTHIA 6 Z2 and HERWIG++ describe the measurements at the detector level equally well. It was found that bin migration effects obtained from simulations with either HERWIG++ or PYTHIA 6 Z2 are similar, and do not exceed 40% at the p_T threshold and 20% for the $\Delta\phi$ distribution.

The correction factors for the $\Delta\phi$ distributions are determined for each of the three Δy bins and each $\Delta\phi$ bin as a ratio of normalised number of bin entries at stable particle leve to that at level (Fig. 1). The correction factors for the average cosines are calculated from two-dimensional $(\Delta\phi, \Delta y)$ distributions as the ratio of the number of entries in each bin at stable particle level to the number at detector level. The obtained correction factors are made smooth with a 2-dimensional fit and used as weights in the determination of the average cosines for every Δy bin. In [32] it was shown that the jet energy resolution for calorimeter jets in Monte Carlo is 6.5-14.9% better than the one in data. These additional corrections are also applied.

6 Measurement uncertainties

The following sources of systematic uncertainty were considered:

1. Jet energy scale uncertainty. The four vectors of the jets were smeared by the jet energy scale uncertainty, which is p_T and η - dependent [32]. The resulting difference of the upper and lower variation define the uncertainty band.

2. Uncertainty of correction factors. The correction factors were determined from PYTHIA6 Z2 and HERWIG++ and averaged for the central value, while the difference was taken as the model uncertainty. An additional uncertainty coming from the limited Monte Carlo statistics was added in quadrature.

3. Jet energy resolution uncertainty in Monte Carlo. The jet energy resolution is different in the Monte Carlo simulation compared to that obtained in data [32], varying between 7.6% and 23.7% depending on η. This difference was accounted for by extra smearing of the four vectors of the jets in the Monte Carlo simulation.

4. Uncertainty of η and ϕ resolutions in Monte Carlo. The angular resolution in the Monte Carlo simulation was varied by $\pm 10\%$. It was found that the resulting uncertainty is negligible compared to the other systematic uncertainties and is therefore neglected.

5. Pileup. The sensitivity of the measurement to pileup was investigated using collision data. In the analysis the number of primary vertices per event is required to be equal to 1. However due to finite primary vertex reconstruction efficiency a residual dependence of observables on pileup may be present. The available datasets were divided into two sets of runs corresponding to different instantaneous bunch luminosities. The observables

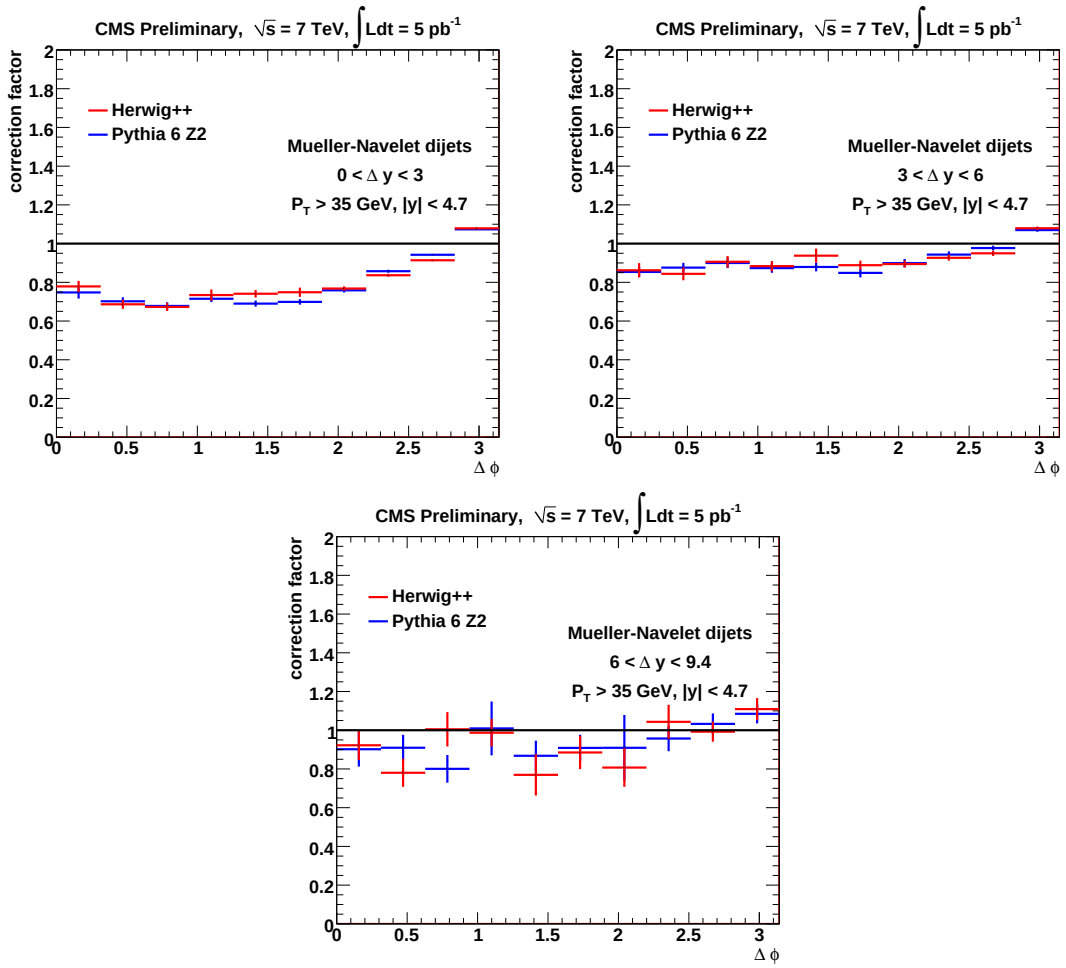

Figure 1: Correction factors for $\Delta\phi$ distributions determined for each of the three Δy bins $\Delta y < 3.0$, $3.0 < \Delta y < 6.0$ and $6.0 < \Delta y < 9.4$, respectively.

obtained from each set of runs were compared, and no dependence on instantaneous luminosity was found.

Table 1: Sources of systematic effects and the associated uncertainties (%). The ranges correspond to the variation of the uncertainty with $\Delta\phi$ or with Δy. For different uncertainty sources, the minimum and maximum values may correspond to different Δy bins. For asymmetric uncertainties the upper and lower limits are shown. Statistical uncertainties are shown for the data.

Observable	JES	JER	Corrections	Total systematic	Statistical
$\Delta\phi(\Delta y < 3.0)$	$^{+(1.5-12.6)}_{-(1.3-8.9)}$	$^{+(0.4-11.3)}_{-(1.1-8.5)}$	$0.3-3.5$	$^{+(2.2-17.2)}_{-(2.1-11.9)}$	$0.2-3.4$
$\Delta\phi(3.0 < \Delta y < 6.0)$	$^{+(0.4-13.8)}_{-(1.3-9.9)}$	$^{+(0.1-7.4)}_{-(0.3-3.6)}$	$0.7-3.0$	$^{+(1.8-15.7)}_{-(2.2-11.0)}$	$0.5-4.6$
$\Delta\phi(6.0 < \Delta y < 9.4)$	$^{+(0.8-38.0)}_{-(1.0-17.9)}$	$^{+(2.5-10.1)}_{-(1.6-11.2)}$	$3.6-13.0$	$^{+(8.6-38.8)}_{-(5.3-29.4)}$	$4.4-19.7$
C_1	$1.0-5.5$	$0.6-3.6$	$0.1-5.4$	$1.0-4.8$	$0.1-3.3$
C_2	$1.5-7.0$	$1.0-8.8$	$0.2-4.0$	$1.7-8.0$	$0.2-2.8$
C_3	$1.8-7.2$	$1.5-15.0$	$0.3-4.1$	$2.2-8.2$	$0.2-2.8$
C_2/C_1	$0.9-9.6$	$0.4-5.6$	$0.2-9.5$	$1.0-14.7$	$0.1-7.4$
C_3/C_2	$0.7-12.5$	$0.2-7.0$	$0.3-15.1$	$0.8-18.4$	$0.2-7.7$

The total systematic uncertainty is obtained by summing in quadrature the individual uncertainties, which are summarised in Tab. 1.

7 Results

The measured $\Delta\phi$ distributions in the three rapidity intervals $\Delta y < 3.0$, $3.0 < \Delta y < 6.0$ and $6.0 < \Delta y < 9.4$ are shown in the left column of Figs. 2, 3, 4, together with the predictions from various MC generators. The systematic uncertainties are shown as a band around the data points. The measurement shows a high level of correlation in the $\Delta y < 3.0$ (Fig. 2) bin, while the $\Delta\phi$ distribution is less peaked at $\Delta\phi \sim \pi$ for $6.0 < \Delta y < 9.4$ (Fig. 4). This shows the increasing influence of higher order corrections for larger Δy. In the right column of Figs. 2, 3, 4 the distributions normalised to the data are shown.

In the central rapidity interval $\Delta y < 3.0$ (Fig. 2) the LL DGLAP based MC generators PYTHIA 6 Z2 and HERWIG++ 2.5 show a fair description of the data within the experimental uncertainties. The LL DGLAP based MC generators PYTHIA 8 4C and SHERPA 1.4, with parton matrix elements matched to LL DGLAP parton showers, exhibit deviations from the data beyond experimental uncertainties at small and intermediate $\Delta\phi$. In the intermediate ($3.0 < \Delta y < 6.0$) and large ($6.0 < \Delta y < 9.4$) rapidity intervals, all the considered LL DGLAP-based MC generator predictions for $\Delta\phi$ distributions show deviations from the data beyond the experimental uncertainties (Figs. 2, 3). However, χ^2 analysis showed that HERWIG++ provides the best and overall satisfactory description of the data. The BFKL-inspired generator CASCADE 2 predicts far too strong decorrelations in the central and intermediate rapidity intervals (no results are shown for the $6.0 < \Delta y < 9.4$ interval due to technical limitations of the MC generator).

The average cosines decrease with increasing Δy in the data, as shown in Figs. 5, 6 and 7. Also shown are predictions obtained from various MC generators.

In the left column of the Figs. 5, 6, 7, the measured average cosine are compared to the LL parton shower Monte Carlo generators PYTHIA 6 Z2, HERWIG++ 2.5 and PYTHIA 8 4C.

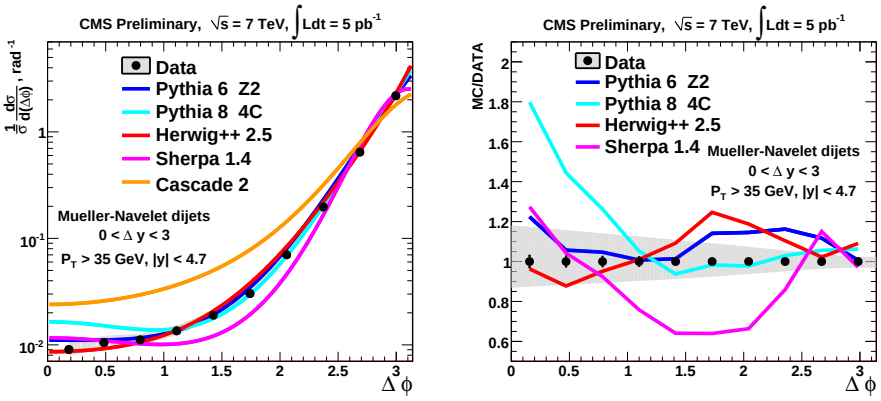

Figure 2: Distribution of azimuthal angle difference, $\Delta\phi$, between MN jets in rapidity interval $\Delta y < 3.0$ and its comparison to the predictions from LL based MC generators PYTHIA 6 Z2, PYTHIA 8 4C, HERWIG++ 2.5, SHERPA 1.4 and LL BFKL motivated MC generator CASCADE 2.

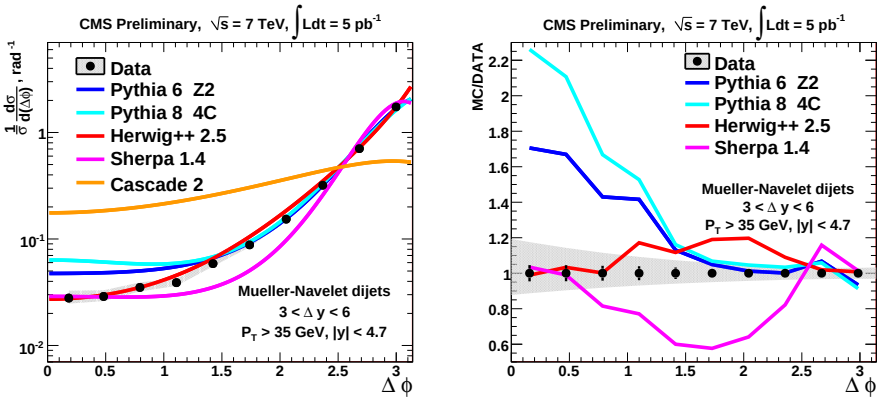

Figure 3: Distribution of azimuthal angle difference, $\Delta\phi$, between MN jets in rapidity interval $3.0 < \Delta y < 6.0$ and its comparison to the predictions from LL based MC generators PYTHIA 6 Z2, PYTHIA 8 4C, HERWIG++ 2.5, SHERPA 1.4 and LL BFKL motivated MC generator CASCADE 2.

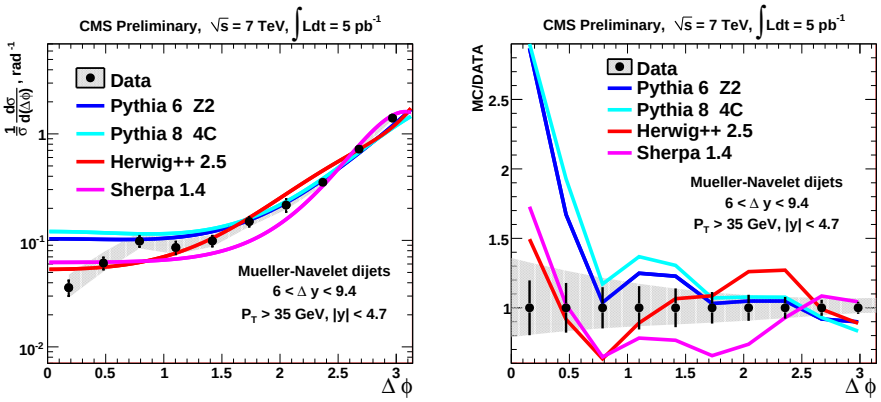

Figure 4: Distribution of azimuthal angle difference, $\Delta\phi$, between MN jets in rapidity interval $6.0 < \Delta y < 9.4$ and its comparison to the predictions from LL based MC generators PYTHIA 6 Z2, PYTHIA 8 4C, HERWIG++ 2.5 and SHERPA 1.4. Prediction from LL BFKL motivated MC generator CASCADE 2 is not shown due to its technical limitations.

In the right column of Figs. 5, 6, 7 the measurements are compared to CASCADE 2, to the analytic NLL BFKL calculations for Δy range from 4 to 9.4 [21], and to the matrix element generator SHERPA 1.4. Note, that CASCADE 2 predictions are available only for not too large Δy (see above) and stable results of the analytic NLL BFKL calculations at the parton level [21] are obtained only for $\Delta y > 4$ range. [1]

The comparison of the measurement with theory predictions can be summarised as follows (see Figs. 5, 6, 7):

- PYTHIA 6 Z2 and PYTHIA 8 4C show a slightly stronger decorrelation for the average cosine at large Δy than in the data. For $< cos(2(\pi - \Delta\phi)) >$ and $< cos(2(\pi - \Delta\phi)) >$ PYTHIA 6 Z2 and PYTHIA 8 4C show a fair agreement with the data;
- HERWIG++ 2.5 shows a satisfactory agreement with the data on the average cosine. For $< cos(2(\pi - \Delta\phi)) >$ and $< cos(2(\pi - \Delta\phi)) >$ HERWIG++ 2.5 begins to show a stronger decorrelation at large Δy than is observed in the data;
- SHERPA underestimates the azimuthal decorrelation at large Δy for the measured the average cosines;
- CASCADE 2 strongly overestimates the azimuthal decorrelation at large Δy for the measured the average cosines;
- the analytic NLL BFKL calculations performed on the parton level [21] tend to underestimate the azimuthal decorrelation compared to the data. However, the very large uncertainties of the NLL BFKL approximation do not allow a firm conclusion to be drawn.

As mentioned in the introduction the ratios of cosines are expected to be more sensitive [18] to BFKL effects than the average cosines and $\Delta\phi$-distributions, because of a cancellation of DGLAP contributions. The measured ratios C_2/C_1 and C_3/C_2 as a function Δy are shown in Fig. 8 and Fig. 9.

The following observations can be drawn from a comparison with MC generators (see Figs. 8, 9):

- PYTHIA 6 Z2 and PYTHIA 8 4C underestimate the azimuthal decorrelation for the average cosine ratio C_2/C_1 at large Δy compared to the measurement but are consistent with the data for C_3/C_2 within the rather large experimental uncertainties;
- HERWIG++ 2.5 overestimates the azimuthal decorrelation for the average cosine ratios C_2/C_1 and C_3/C_2 at large Δy;
- SHERPA underestimates the azimuthal decorrelation at large Δy for the average cosine ratio C_2/C_1 but is consistent with the data for C_3/C_2 within the rather large experimental uncertainties;
- CASCADE 2 strongly overestimates the azimuthal decorrelation at large Δy for the average cosine ratio C_2/C_1 and C_3/C_2;
- the analytic NLL BFKL calculation performed on the parton level [21] is consistent with the data on C_3/C_2 within the experimental and theoretical uncertainties.

The azimuthal angle decorrelation can also depend on effects coming from polar angle ordering (AO) in the parton showering and multiparton interactions (MPI). The polar angle ordering

[1] The large and asymmetric uncertainties in the NLL BFKL predictions [21] are caused by omitting subleading terms, which have been obtained by variation of the parameters of the NLL BFKL approximation (renormalisation, factorisation and Regge scales).

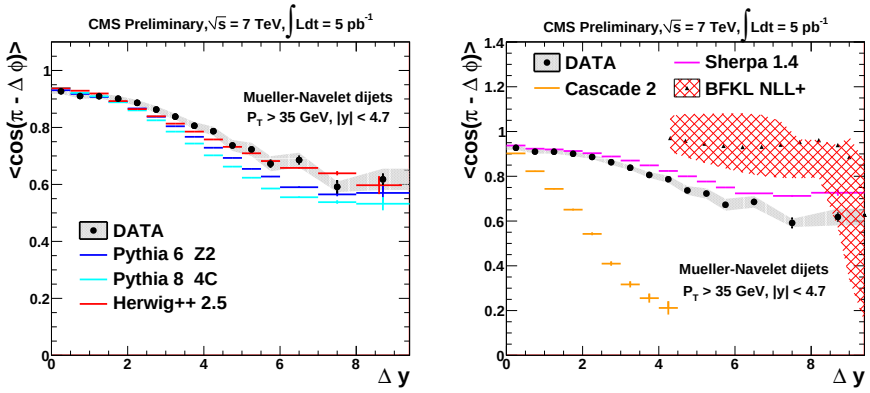

Figure 5: Average $< \cos \pi - \Delta\phi >$ as a function of Δy compared to LL DGLAP MC generators is shown on the left. On the right, comparison to MC generator SHERPA with parton matrix elements matched to LL DGLAP parton shower, LL BFKL inspired generator CASCADE and analytic NLL BFKL calculations on the parton level ($\Delta y > 4$) is presented.

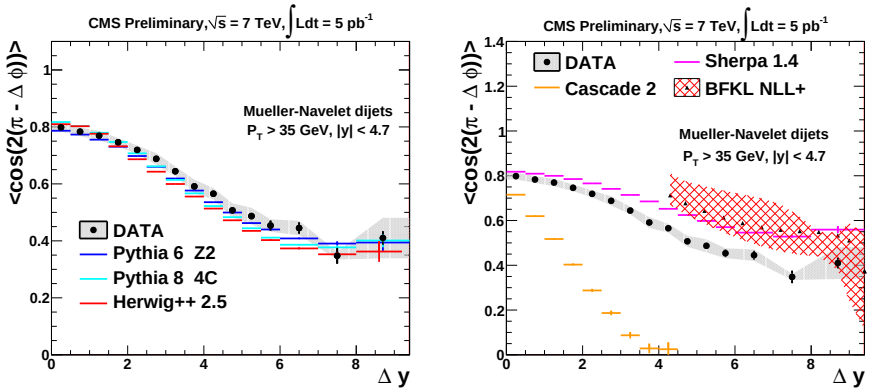

Figure 6: Average $< \cos(2(\pi - \Delta\phi)) >$ as a function of Δy compared to LL DGLAP MC generators is shown on the left. On the right, comparison to MC generator SHERPA with parton matrix elements matched to LL DGLAP parton shower, LL BFKL inspired generator CASCADE and analytic NLL BFKL calculations on the parton level ($\Delta y > 4$) is presented.

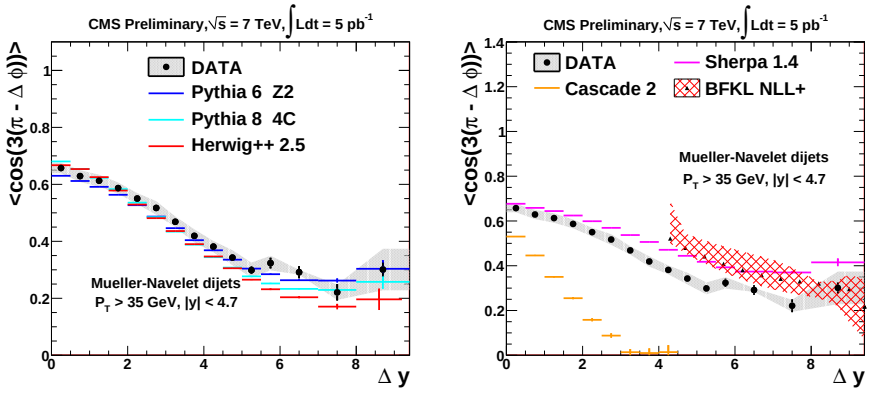

Figure 7: Average $< \cos(3(\pi - \Delta\phi)) >$ as a function of Δy compared to LL DGLAP MC generators is shown on the left. On the right, comparison to MC generator SHERPA with parton matrix elements matched to LL DGLAP parton shower, LL BFKL inspired generator CASCADE and analytic NLL BFKL calculations on the parton level ($\Delta y > 4$) is presented.

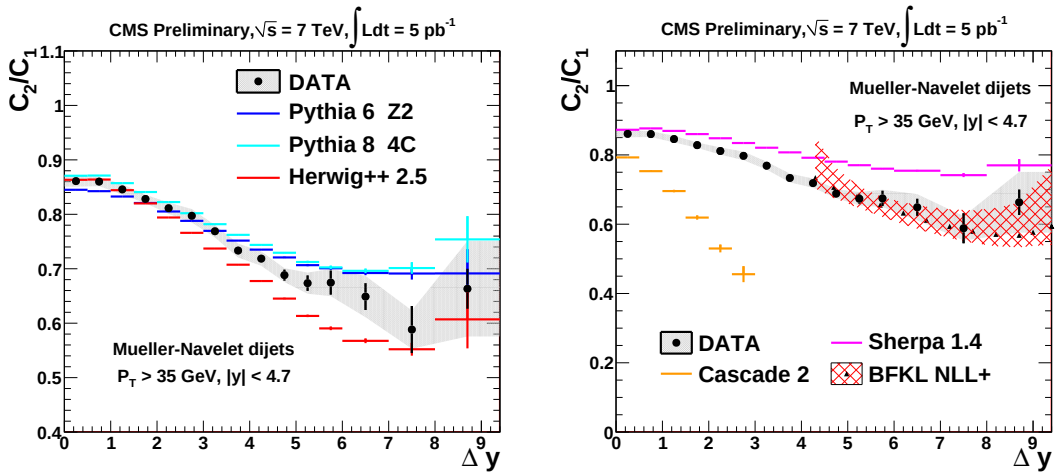

Figure 8: On the left measured ratio C_2/C_1 as a function of rapidity difference Δy is compared to LL DGLAP parton shower generators. On the right the ratio is compared to MC generator SHERPA with parton matrix element matched to LL DGLAP parton shower, LL BFKL - inspired generator CASCADE and analytic NLL BFKL calculations at the parton level.

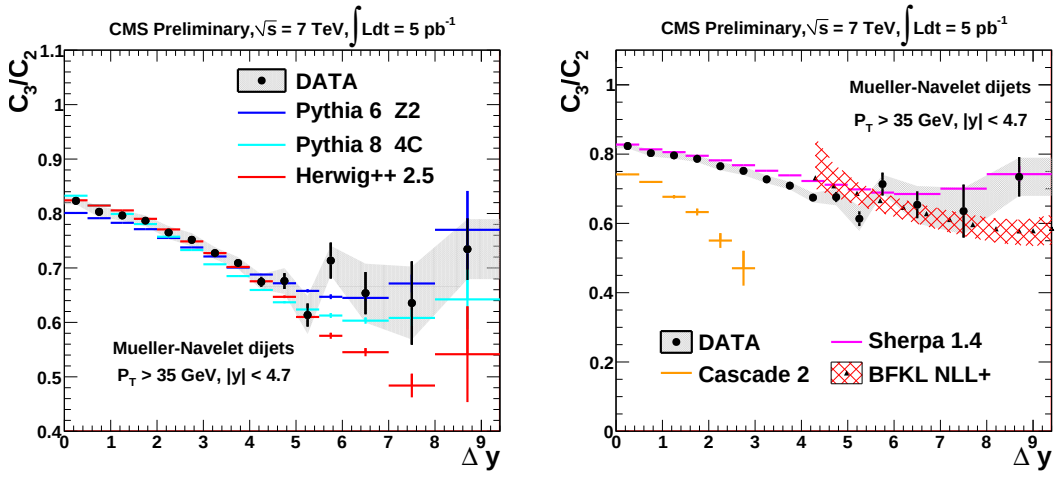

Figure 9: On the left measured ratio C_3/C_2 as a function of rapidity difference Δy is compared to LL DGLAP parton shower generators. On the right the ratio is compared to MC generator SHERPA with parton matrix element matched to LL DGLAP parton shower, LL BFKL - inspired generator CASCADE and analytic NLL BFKL calculations at the parton level.

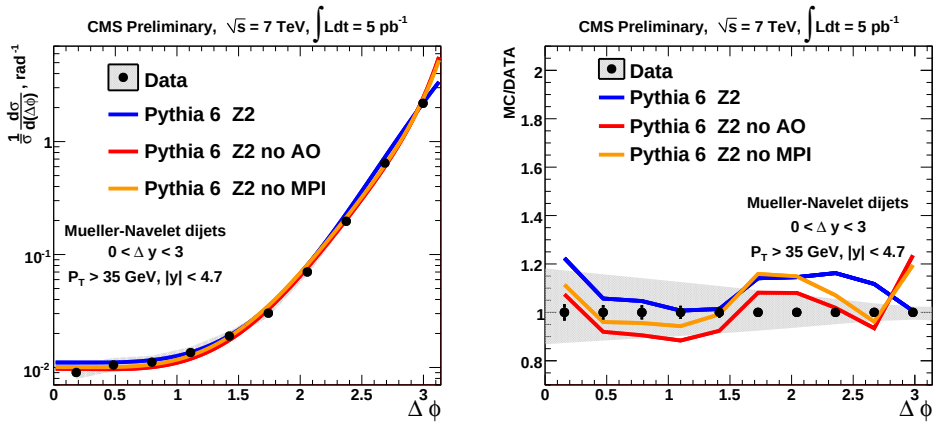

Figure 10: Distributions of azimuthal angle difference (left) between MN jets with $0 < \Delta y < 3$ compared to PYTHIA6 Z2 without multiple parton interaction modeling or without angular ordering for parton shower. Detailed comparison is presented as MC/data ratio (right).

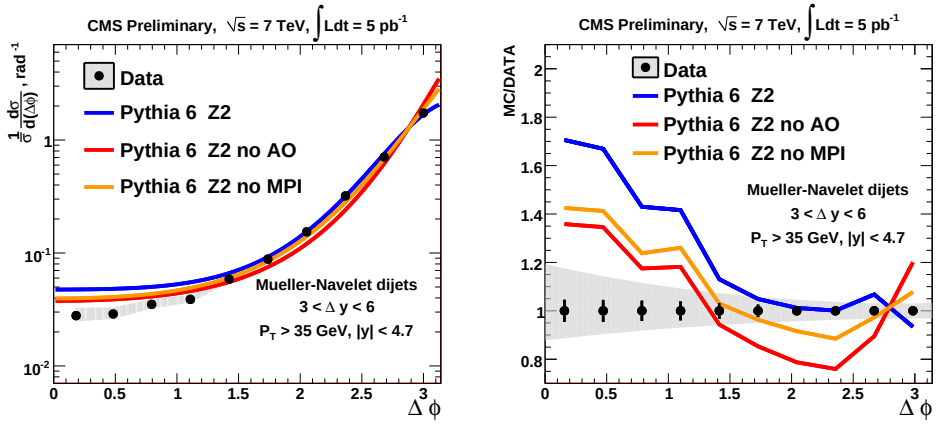

Figure 11: Distributions of azimuthal angle difference (left) between MN jets with $3 < \Delta y < 6$ compared to PYTHIA6 Z2 without multiple parton interaction modeling or without angular ordering for parton shower. Detailed comparison is presented as MC/data ratio (right).

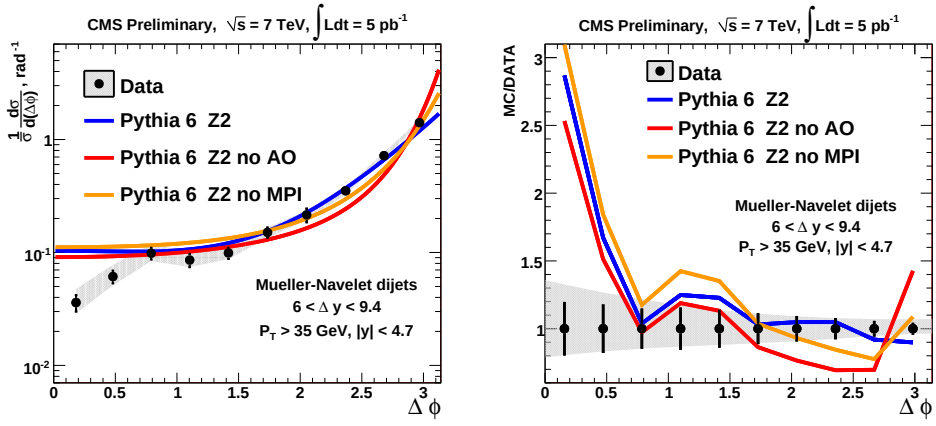

Figure 12: Distributions of azimuthal angle difference (left) between MN jets with $6 < \Delta y < 9.4$ compared to PYTHIA6 Z2 without multiple parton interaction modeling or without angular ordering for parton shower. Detailed comparison is presented as MC/data ratio (right).

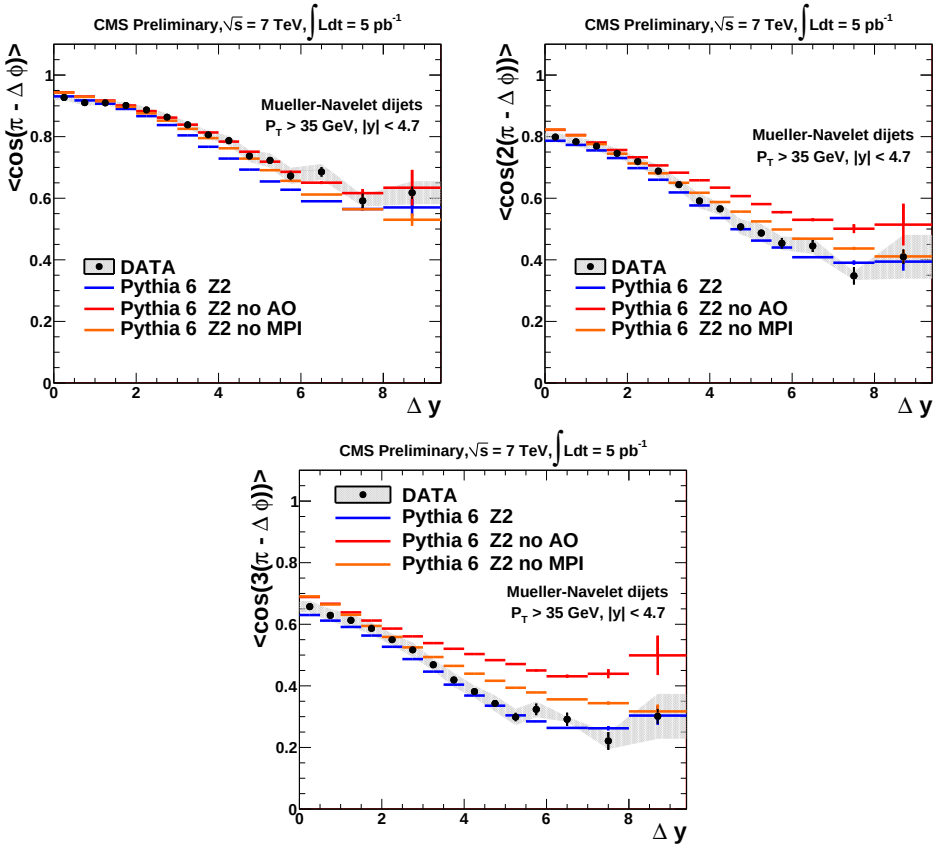

Figure 13: Average $< \cos(\pi - \Delta\phi) >$, $< \cos 2(\pi - \Delta\phi) >$ and $< \cos 3(\pi - \Delta\phi) >$ compared to PYTHIA6 Z2 without multiple parton interaction modeling (left) or without angle ordering for parton shower (right).

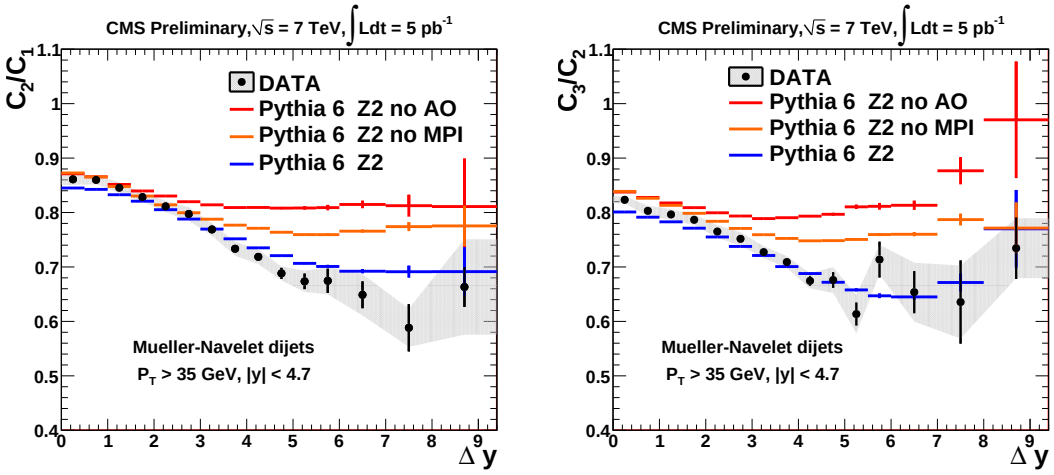

Figure 14: Measured ratios C_2/C_1 (left) and C_3/C_2 (right) are compared to PYTHIA6 Z2 with modified multiple parton interaction modeling and different ordering of parton emissions.

causes parton emissions at larger angles to be vetoed during parton showering, and effectively takes into account extra colour quantum interference beyond the LL DGLAP approach. This leads to an enhanced probability for emission of partons at smaller polar angles and, hence, to increased azimuthal de-corellations at large rapidities.

To estimate the impact of AO the corresponding option was turned on/off in PYTHIA 6. The AO condition is built in to MC generators such as PYTHIA 8 and HERWIG++ 2.5 as a colour coherence effect.

Multiparton interactions, which can produce additional uncorrelated jets, are another source of azimuthal angle decorrelations. By default, MPI effects are included in the MC generators PYTHIA 6, PYTHIA 8 , HERWIG++ 2.5, and SHERPA 1.4. To study this effect, the corresponding option in PYTHIA 6 was used to disable MPI.

The measurements are compared with the MC predictions without AO and without MPI in Fig. 10, 11, 12. Figure 13 demonstrates that average cosines are sensitive to the parton ordering scheme in the parton shower and to the details of MPI modelling. A good description of the data requires polar angle ordering in parton showering.

Another potential source of azimuthal angle decorrelations is non-perturbative hadronisation of the produced partons. The effects of non-perturbative hadronisation were estimated by comparison of observables at the parton and stable particle levels, as obtained with PYTHIA6 Z2, giving an increase of the correlation of up to 10 %. The size of the effect is less than the experimental systematics uncertainties, thus it justifies a direct comparison of the analytical NLL BFKL calculations [21] performed on the parton level with the measured observables.

8 Conclusion

The first measurement of the azimuthal angle decorrelations of Mueller-Navelet dijets with a rapidity separation of up to $\Delta y = 9.4$, in proton-proton collisions at $\sqrt{s} = 7\,\text{TeV}$, is presented. The measuremed observables include azimuthal angle distributions, average cosines of the azimuthal angle, double and triple angles, and ratios of the average cosines.

The predictions of the DGLAP-based MC generator HERWIG++ 2.5 demonstrate satisfactory agreement with the data for all measured observables. Other MC generators of this type - PYTHIA 6 Z2, PYTHIA 8 4C and SHERPA 1.4 do not provide a good description of all measurements.

The average cosine ratios are particularly sensitive to the details of parton showering and multiparton interaction: without implementing polar angle ordering in parton showering and multiparton interactions the considered DGLAP MC generators show significant deviations from the data.

CASCADE 2, which has incorporated essential elements of LL BFKL but is missing some elements of collinear factorisation of DGLAP approach, predicts too strong azimuthal decorrelations.

Analytical BFKL calculations performed at next-to-leading logarithmic (NLL) approximation provide a satisfactory description of the data for the average cosine ratios.

The observed disagreement of LL DGLAP MC generators without polar angle ordering in parton showering may be considered as a hint that the kinematical domain of the present study lies in transition between the regions described by the DGLAP and BFKL approaches. For further

investigations of possible manifestations of BFKL effects in these observables, data at higher energies are needed.

Acknowledgements

We would like to thank Bertrand Ducloué, Lech Szymanowski and Samuel Wallon for providing the full NLL BFKL analytical predictions.

We congratulate our colleagues in the CERN accelerator departments for the excellent performance of the LHC machine. We thank the technical and administrative staff at CERN and other CMS institutes, and acknowledge support from: FMSR (Austria); FNRS and FWO (Belgium); CNPq, CAPES, FAPERJ, and FAPESP (Brazil); MES (Bulgaria); CERN; CAS, MoST, and NSFC (China); COLCIENCIAS (Colombia); MSES (Croatia); RPF (Cyprus); MoER, SF0690030s09 and ERDF (Estonia); Academy of Finland, MEC, and HIP (Finland); CEA and CNRS/IN2P3 (France); BMBF, DFG, and HGF (Germany); GSRT (Greece); OTKA and NKTH (Hungary); DAE and DST (India); IPM (Iran); SFI (Ireland); INFN (Italy); NRF and WCU (Korea); LAS (Lithuania); CINVESTAV, CONACYT, SEP, and UASLP-FAI (Mexico); MSI (New Zealand); PAEC (Pakistan); MSHE and NSC (Poland); FCT (Portugal); JINR (Armenia, Belarus, Georgia, Ukraine, Uzbekistan); MON, RosAtom, RAS and RFBR (Russia); MSTD (Serbia); MICINN and CPAN (Spain); Swiss Funding Agencies (Switzerland); NSC (Taipei); TUBITAK and TAEK (Turkey); STFC (United Kingdom); DOE and NSF (USA).

References

[1] V.N. Gribov, L.N. Lipatov, "Deep inelastic e p scattering in perturbation theory", *Sov. J. Nucl. Phys.* **15** (1972) 438–450.

[2] V.N. Gribov, L.N. Lipatov, "e+ e- pair annihilation and deep inelastic e p scattering in perturbation theory", *Sov. J. Nucl. Phys.* **15** (1972) 675–684.

[3] L.N. Lipatov, "The parton model and perturbation theory", *Sov. J. Nucl. Phys.* **20** (1975) 94–102.

[4] G. Altarelli, G. Parisi, "Asymptotic Freedom in Parton Language", *Nucl. Phys. B* **126** (1977) 298.

[5] Y.L. Dokshitzer, "Calculation of the Structure Functions for Deep Inelastic Scattering and e+ e- Annihilation by Perturbation Theory in Quantum Chromodynamics", *Sov. Phys. JETP* **46** (1977) 641–653.

[6] E.A. Kuraev, L.N. Lipatov, V.S. Fadin, "Multi - Reggeon Processes in the Yang-Mills Theory", *Sov. Phys. JETP* **44** (1976) 443–450.

[7] E.A. Kuraev, L.N. Lipatov, V.S. Fadin, "The Pomeranchuk Singularity in Nonabelian Gauge Theories", *Sov. Phys. JETP* **45** (1977) 199–204.

[8] I.I. Balitsky, L.N. Lipatov, "The Pomeranchuk Singularity in Quantum Chromodynamics", *Sov. J. Nucl. Phys.* **28** (1978) 822–829.

[9] A.H. Mueller, H. Navelet, "An Inclusive Minijet Cross-Section and the Bare Pomeron in QCD", *Nucl. Phys. B* **282** (1987) 727.

[10] V. Del Duca and C. R. Schmidt, "Mini - jet corrections to Higgs production", *Phys. Rev. D* **49** (1994) 177–182, doi:10.1103/PhysRevD.49.177, arXiv:hep-ph/9305346.

[11] W. J. Stirling, "Production of jet pairs at large relative rapidity in hadron hadron collisions as a probe of the perturbative pomeron", *Nucl. Phys. B* **423** (1994) 56–79, doi:10.1016/0550-3213(94)90565-7, arXiv:hep-ph/9401266.

[12] S. Abachi *et al.* [D0 Collaboration], "The Azimuthal decorrelation of jets widely separated in rapidity", *Phys. Rev. Lett.* **77** (1996) 595–600.

[13] S. Abbott *et al.* [D0 Collaboration], "Probing BFKL dynamics in the dijet cross section at large rapidity intervals in $p\bar{p}$ collisions at $\sqrt{s} = 1800$ GeV and 630-GeV", *Phys. Rev. Lett.* **84** (2000) 5722–5727.

[14] ATLAS Collaboration, "Measurement of dijet production with a veto on additional central jet activity in pp collisions at $\sqrt{s} = 7$ TeV using the ATLAS detector", *JHEP* **1109** (2011) 053, doi:10.1007/JHEP09(2011)053, arXiv:1107.1641.

[15] CMS Collaboration, "Ratios of dijet production cross sections as a function of the absolute difference in rapidity between jets in proton-proton collisions at $\sqrt{s} = 7$ TeV", *Eur. Phys. J. C* **72** (2012) 2216, doi:10.1140/epjc/s10052-012-2216-6, arXiv:1204.0696.

[16] V. T. Kim and G. B. Pivovarov, "BFKL QCD pomeron in high-energy hadron collisions: Inclusive dijet production", *Phys. Rev. D* **53** (1996) 6–10, doi:10.1103/PhysRevD.53.6, arXiv:hep-ph/9506381.

[17] A. Sabio Vera and F. Schwennsen, "The Azimuthal decorrelation of jets widely separated in rapidity as a test of the BFKL kernel", *Nucl. Phys. B* **776** (2007) 170–186, doi:10.1016/j.nuclphysb.2007.03.050, arXiv:hep-ph/0702158.

[18] M. Angioni et al., "Dijet Production at Large Rapidity Separation in N=4 SYM", *Phys. Rev. Lett.* **107** (2011) 191601, doi:10.1103/PhysRevLett.107.191601, arXiv:hep-th/1106.6172.

[19] B. Ducloué, L. Szymanowski, and S. Wallon, "Mueller-Navelet jets at LHC: the first complete NLL BFKL study", *PoS* **QNP2012** (2012) 165, arXiv:1208.6111.

[20] S. Brodsky et al., "The QCD pomeron with optimal renormalization", *JETP Lett.* **70** (1999) 155–160, doi:10.1134/1.568145, arXiv:hep-ph/9901229.

[21] B. Ducloué, L. Szymanowski, and S. Wallon, "Confronting Mueller-Navelet jets in NLL BFKL with LHC experiments at 7 TeV", arXiv:hep-ph/1302.7012.

[22] M. Cacciari, G.P.Salam and G.Soyez, "The anti-kt jet clustering algorithm", *JHEP* **04** (2008).

[23] M. Cacciari and G. P. Salam, "Dispelling the N^3 myth for the kT jet-finder", *Phys. Lett. B* **641** (2006) 57, doi:10.1016/j.physletb.2006.08.037, arXiv:hep-ph/0512210.

[24] T. Sjöstrand, S. Mrenna, P. Skands, "Pythia 6.4 Physics and Manual", *JHEP* **05** (2006) 026.

[25] R. Field, "Min-Bias and the Underlying Event at the LHC", *Acta Phys. Polon. B* **42** (2011) 2631, arXiv:hep-ph/1110.5530.

[26] M. Bahr *et al.*, "HERWIG++ Physics and Manual", *Eur.Phys.J.* **C58** (2008) 639–707.

[27] T. Sjöstrand, S. Mrenna, and P. Skands, "A Brief Introduction to PYTHIA 8.1", *Comput. Phys. Commun.* **178** (2008) 852, doi:10.1016/j.cpc.2008.01.036.

[28] R. Corke and T. Sjöstrand, "Interleaved Parton Showers and Tuning Prospects", *JHEP* **3** (2011) 32, doi:10.1007/JHEP03(2011)032, arXiv:1011.1759.

[29] P. E. Freeman, S. Doe, and A. Siemiginowska, "Sherpa: a mission-independent data analysis application", arXiv:astro-ph/0108426.

[30] H. Jung et al., "The CCFM Monte Carlo generator CASCADE version 2.2.03", *Eur. Phys. J. C* **70** (2010) 1237–1249, doi:10.1140/epjc/s10052-010-1507-z, arXiv:1008.0152.

[31] CMS Collaboration, "The CMS experiment at the CERN LHC", *JINST* **0803:S08004** (2008).

[32] CMS Collaboration, "Determination of Jet Energy Calibration and Transverse Momentum Resolution in CMS", *JINST* **6** (2011) P11002, doi:10.1088/1748-0221/6/11/P11002, arXiv:1107.4277.

[33] CMS Collaboration, "Jet Performance in pp Collisions at $\sqrt{s}$=7 TeV", CMS Physics Analysis Summary CMS-PAS-JME-10-003, (2010).

[34] CMS Collaboration, "Tracking and Primary Vertex Results in First 7 TeV Collisions", CMS Physics Analysis Summary CMS-PAS-TRK-10-005, (2010).

[35] CMS Collaboration, "Calorimeter Jet Quality Criteria for the First CMS Collision Data", *CMS Physics Analysis Summary* **CMS-PAS-JME-09-008** (2010).

[36] S. Agostinelli *et al.*, "Geant4 - A Simulation Toolkit", *Nucl. Inst. Meth. A* **506** (2003) 250–303.